Supporting Information

Heterostructure LDH/oxides as p-n type Electrocatalyst for the alkaline Water Splitting: An Experimental Assessment via Temperature-dependent Study

Hariharan N Dhandapani,[†‡] Kaveri Senthivel,[†‡] Madheshkumar R,[†‡] B. Ramesh Babu[†‡*] and Subrata Kundu[†‡*]

[†]*Academy of Scientific and Innovative Research (AcSIR), Ghaziabad-201002, India.*

[‡]*Electrochemical Process Engineering (EPE) Division, CSIR-Central Electrochemical Research Institute (CECRI), Karaikudi-630003, Tamil Nadu, India.*

**E-mail:* brbabu@cecri.res.in; skundu.cecri@csir.res.in; kundu.subrata@gmail.com;
Phone/Fax: (+ 91) 4565-241487.

This file contains **29** pages of the details of reagents, electrochemical results, electrochemical characterizations, and characterizations like post-HR-TEM, FE-SEM, and EDS spectra results are provided

Table S1: Reagents and Instruments:

The source, company, and purity of the chemicals are given as follows:

S.No	Chemicals	Company	Purity
1	Manganese (II) chloride ($MnCl_2$)	Thermoscientific	98%
2	Urea	ThermoFisher Scientific	99%
3	Ammonium Fluoride (NH_4F)	Sisco Research Laboratory (P) Ltd.	98%
4	Ferric chloride ($FeCl_3$)	Alfa Aesar	97%
5	Acetone	ThermoFisher Scientific	99 %
6	Ethanol	Fine chemical	99.9 %
7	Hydrochloric acid (HCl)	ThermoFisher Scientific	35-37%
9	Ni foam	Sigma-Aldrich	99.9%
10	Tetramethyl ammonium hydroxide	ThermoScientific	99.9%

Ni foam was used after surface cleaning. Characterization of the catalyst was done by HR-TEM, (Tecnai^{TM} G^2 TF20), operating at an accelerating voltage of 200 kV and elemental color mapping by Talos F-200-S with HAADF. Energy Dispersive X-ray Spectroscopy (EDS) analysis was performed by SUPRA 55VP Carl Zeiss with a separate EDS detector. Scanning Electron Microscopy (SEM) analysis was carried with a Hitachi, Japan (Model S-3000H) having magnification varying from 30X to 300 KX with the accelerating voltage ~ 0.3 to 30 kV. XRD analysis was carried out with a scanning rate of 5° min^{-1} in the 2θ range 10-90° using a Rigaku X-ray powder diffractometer (XRD) with Cu K_α radiation (λ = 0.154 nm). LASER Raman spectroscopic measurements were carried out by green emitting semiconductor as a laser source of 532 nm. For Raman experiment the excitation light intensity is about approximately 10 mW with a spectral collection of time of 1 sec. The integration time for our measurement was set to be 10 s. The electrochemical analyzer AURT-M204 was used for all electrochemical characterizations.[1] Hg/HgO reference electrode (1M KOH) from CH

instruments and platinum as counter electrode from Alfa-Aesar were used throughout the electrochemical studies. The entire experiments were conducted using deionised water. The overall potential data was obtained by utilising Hg/HgO (reference electrode), which was converted into an RHE (E_{RHE}) scale by the Nernst equation

$$E_{RHE} = E_{ref} + 14 \times 0.059 + 0.098 \ldots\ldots\ldots\ldots\ldots\ 1$$

Over potential (η) value of MnFe-LDH/Mn_2O_3 to attain a current density of 50 mA/cm^2 is calculated by the following equation:

$$\eta = E_{RHE} - 1.23\ V\ (\text{for OER}) \ldots\ldots\ldots\ldots\ldots\ 2$$

The Tafel equation was fitted to match η vs. log (current density) after determining the Tafel slope from data of the LSV polarization curve.

$$\eta = a + b \times \log (j) \ldots\ldots\ldots\ldots\ldots\ 3$$

where j-current density, b-Tafel slope value. To carry out Electrochemical impedance spectroscopy (EIS) measurements the frequency ranges chosen from 10^5 to 0.1 Hz at 325 mV of overpotential value for OER. Also, Operando-EIS study was performed by using a carbon cloth (CC) electrode-working electrode at a various applied potential. The double layer capacitance (C_{dl}) value can be calculated by evaluating as given below:

$$\Delta J = \nu \times C_{dl} \quad \ldots\ldots\ldots\ 4$$

ΔJ - current in double-layer capacitance obtaining from scan-rates (v) in the non-faradic potential region.[2]

For the RRDE experiment, 4 mg of MnFe-LDH/Mn_2O_3 catalyst was added to a solution containing 200 µL of ethanol, 750 µL of H_2O, and 50 µL of 5% Nafion solution. To prepare a homogeneous catalyst ink mixture was sonicated for 20 min. Later, 15 µL of homogeneous ink

was drop-casted over the GC disk of RRDE set up with an effective surface area of ≈0.197 cm^2. The Pt ring was used with a constant potential of -0.6 V versus RHE to reduce the as-formed O_2 in situ.[3] The FE was calculated from the ratio of the ring current to the disk using the following expression:

$$FE = I_{ring} / (I_{disk} \times N) \times 100 \quad \ldots\ldots\ldots\ldots\ldots\ldots 5$$

where, "I_{ring}" and "I_{disk}" are the ring and disk current density in mA cm^{-2}, respectively; "N" is the collection efficiency having a constant value of 0.247.

Synthesis route of Mn_2O_3/NF:

Initially, the NF was cut into 0.5 × 4 cm^2 and cleaned with 1 M HCl, distilled water, acetone and ethanol for almost 20 minutes. Mn_2O_3 was made over NF by one-step hydrothermal and annealing process. For the synthesis of Mn_2O_3 over NF, 5 mmol of $MnCl_2$, 25 mmol of Urea, and 10 mmol of NH_4F were dissolved in 35 ml of DI water into a Teflon linked autoclave. The NF was also transferred into the autoclave with dissolved solution and sealed properly. The autoclave was kept in the hot air oven at 120 ℃ for 6 h. Later, the in-situ grown $Mn(OH)_2$ over NF was cleaned for several times with DI water and dried at 60°C. The dried ($MnOH_2$)/NF was undergoing an annealing process 350℃ at 4h. The Mn_2O_3 was collected as a black powder sample, as well as nickel foam.

Synthesis of MnFe-LDH/NF:

For comparison, MnFe-LDH/NF was synthesized by using the similar procedure adopted for the synthesis of MnFe-LDH/Mn_2O_3/NF without the inclusion of in-situ grown Mn_2O_3/NF in a Teflon-lined stainless-steel autoclave.

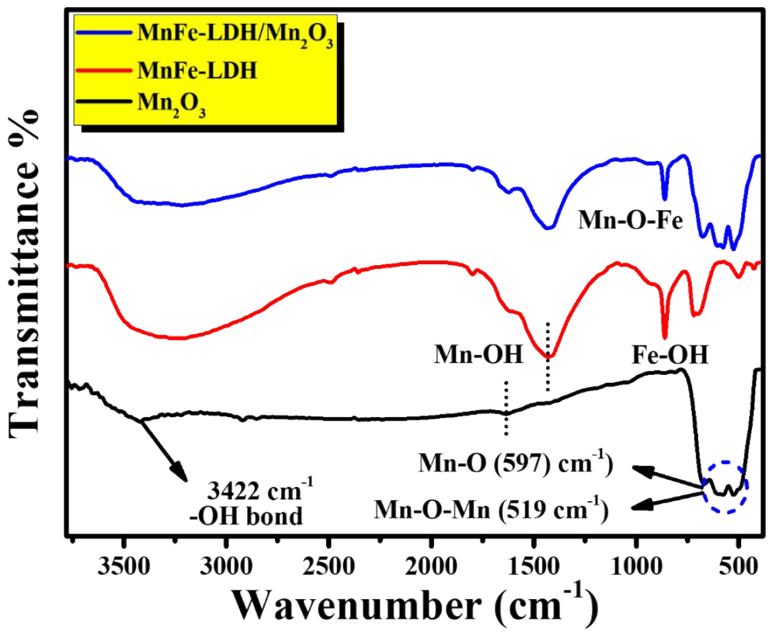

Figure S1: IR spectra for Mn_2O_3, MnFe-LDH and MnFe-LDH/Mn_2O_3.

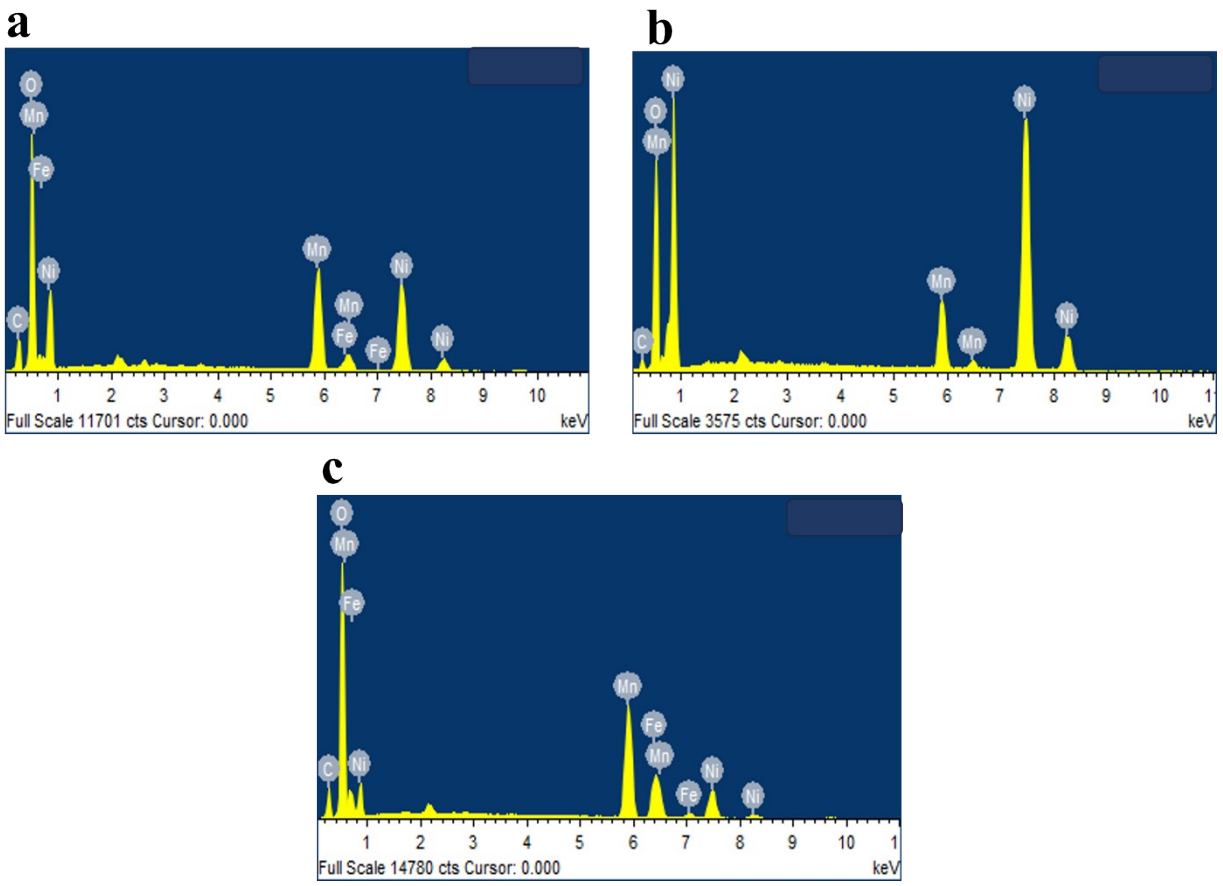

Figure S2: EDS spectrum of (a) Mn_2O_3 (b) MnFe-LDH and (c) MnFe-LDH/Mn_2O_3 from FE-SEM showing the presence of all the expected elements.

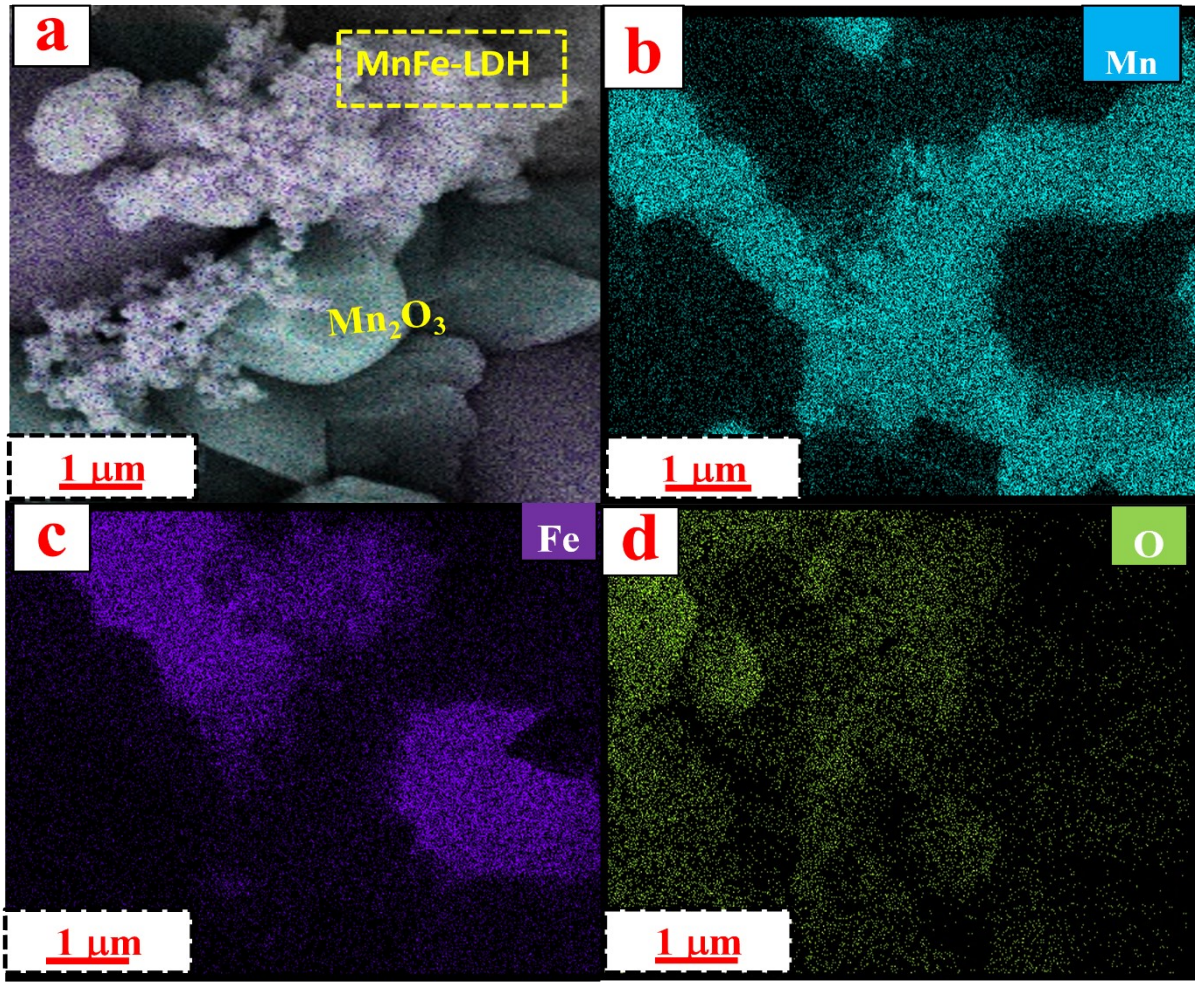

Figure S3: (a) Colour mapping images MnFe-LDH/Mn_2O_3 from FE-SEM, (b-d) Uniform distribution of Mn, Fe, and O elements respectively.

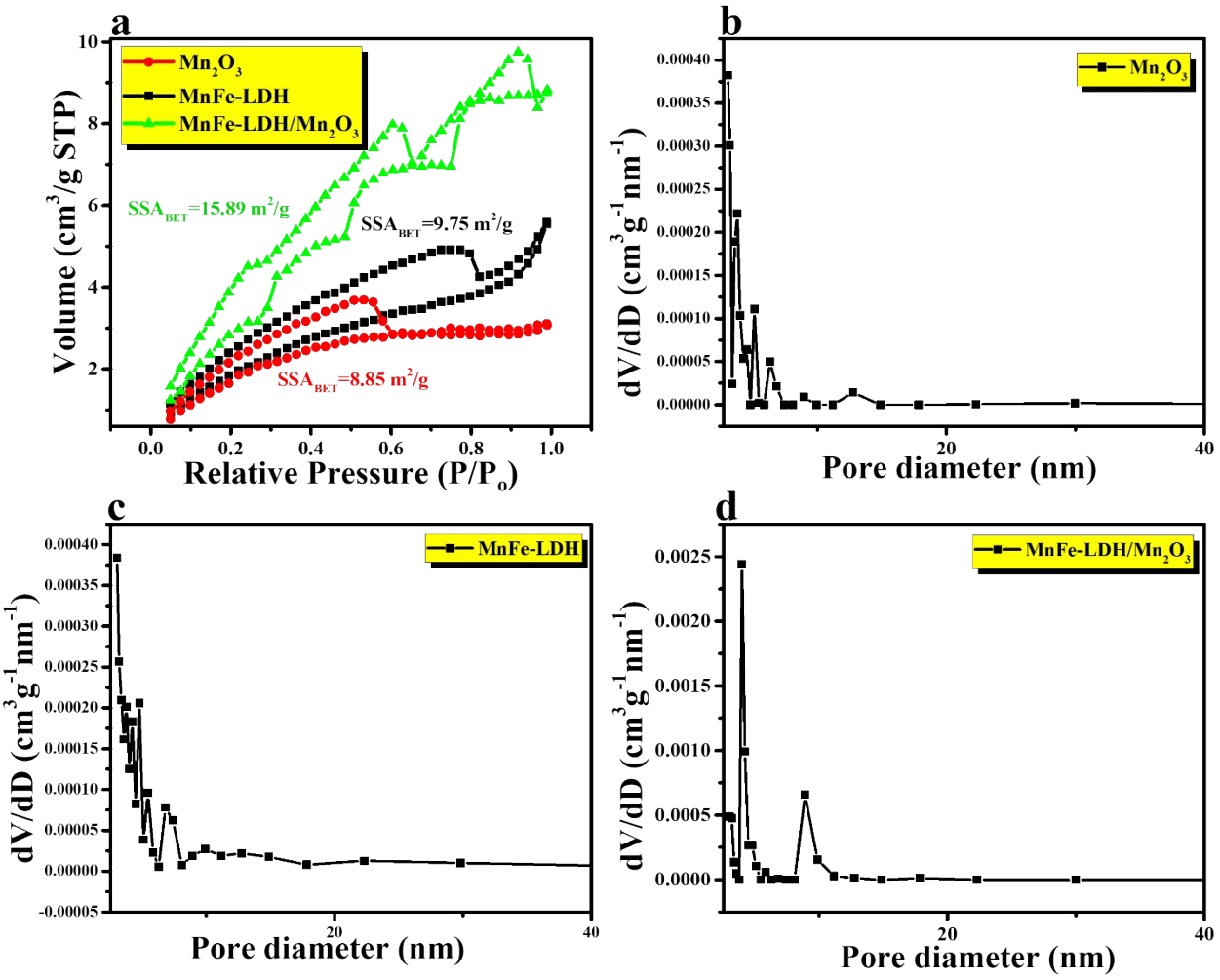

Figure S4: (a) shows N_2 adsorption-desorption of Mn_2O_3, MnFe-LDH and MnFe-LDH/Mn_2O_3 and (b-d) Pore size distribution diagram of Mn_2O_3, MnFe-LDH and MnFe-LDH/Mn_2O_3 respectively.

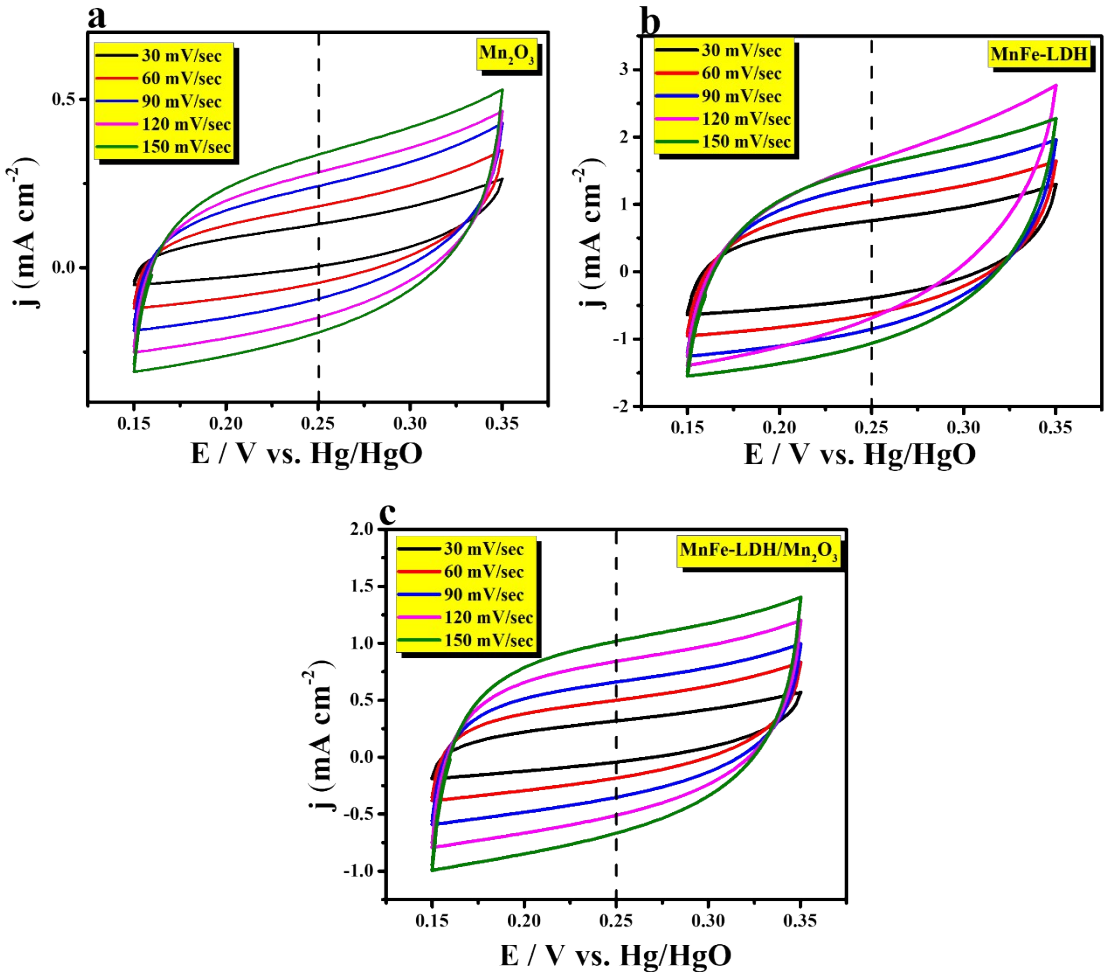

Figure S5: **(a-c)** The electrochemically effective surface area for Mn_2O_3, MnFe-LDH and MnFe-LDH /Mn_2O_3 respectively.

Estimation of the electrochemical double-layer capacitance (C_{dl})

To calculate the electrochemical double-layer capacitance for Mn_2O_3, MnFe-LDH, and MnFe-LDH/Mn_2O_3 the cyclic voltammetry methods were performed with various scan rates ranging from 30 mV/s to 150 mV/s with a step of 30 mV/s. The potential is scanned from 0.15 to 0.35 V vs Hg/HgO where no faradic current was observed. The center of this working potential (i.e., 0.25 V) was selected to calculate ΔJ_0 (vs Hg/HgO). Hence, we plotted the differences in current densities ($\triangle J = J_a - J_c$) at 0.25 V (vs. Hg/HgO) against the scan rates. Hence, the electrochemical double-layer capacitance was calculated using the formula below.

Hence, the electrochemical double-layer capacitance was measured by using the formula

a. For Mn_2O_3 in 1.0 M KOH

$$C_{dl} = \frac{(0.50 - (0.12)(mA/cm^2)}{(150 - 30)(mV/s)} = 3.3 \text{ mFcm}^{-2}$$

b. For MnFe-LDH in 1.0 M KOH

$$C_{dl} = \frac{(2.46 - 1.15)(mA/cm^2)}{(150 - 30)(mV/s)} = 10.91 \text{ mFcm}^{-2}$$

c. For MnFe-LDH/Mn_2O_3 in 1.0 M KOH

$$C_{dl} = \frac{(1.83 - 0.361)(mA/cm^2)}{(150 - 30)(mV/s)} = 12.24 \text{ mFcm}^{-2}$$

The ECSA can be calculated from the C_{dl} according to:

ECSA for Mn_2O_3 $= \frac{3.3\ mFcm^{-2}}{0.04\ mF\ cm^{-2}\ cm_{ECSA}^{2}} = 82.5\ cm_{ECSA}^{2}$

ECSA for MnFe-LDH $= \frac{10.9\ mFcm^{-2}}{0.04\ mF\ cm^{-2}\ cm_{ECSA}^{-2}} = 272.5\ cm_{ECSA}^{2}$

ECSA for $MnFe\text{-}LDH/Mn_2O_3$ $= \frac{12.24\ mFcm^{-2}}{0.04\ mF\ cm^{-2}\ cm_{ECSA}^{-2}} = 306\ cm_{ECSA}^{2}$

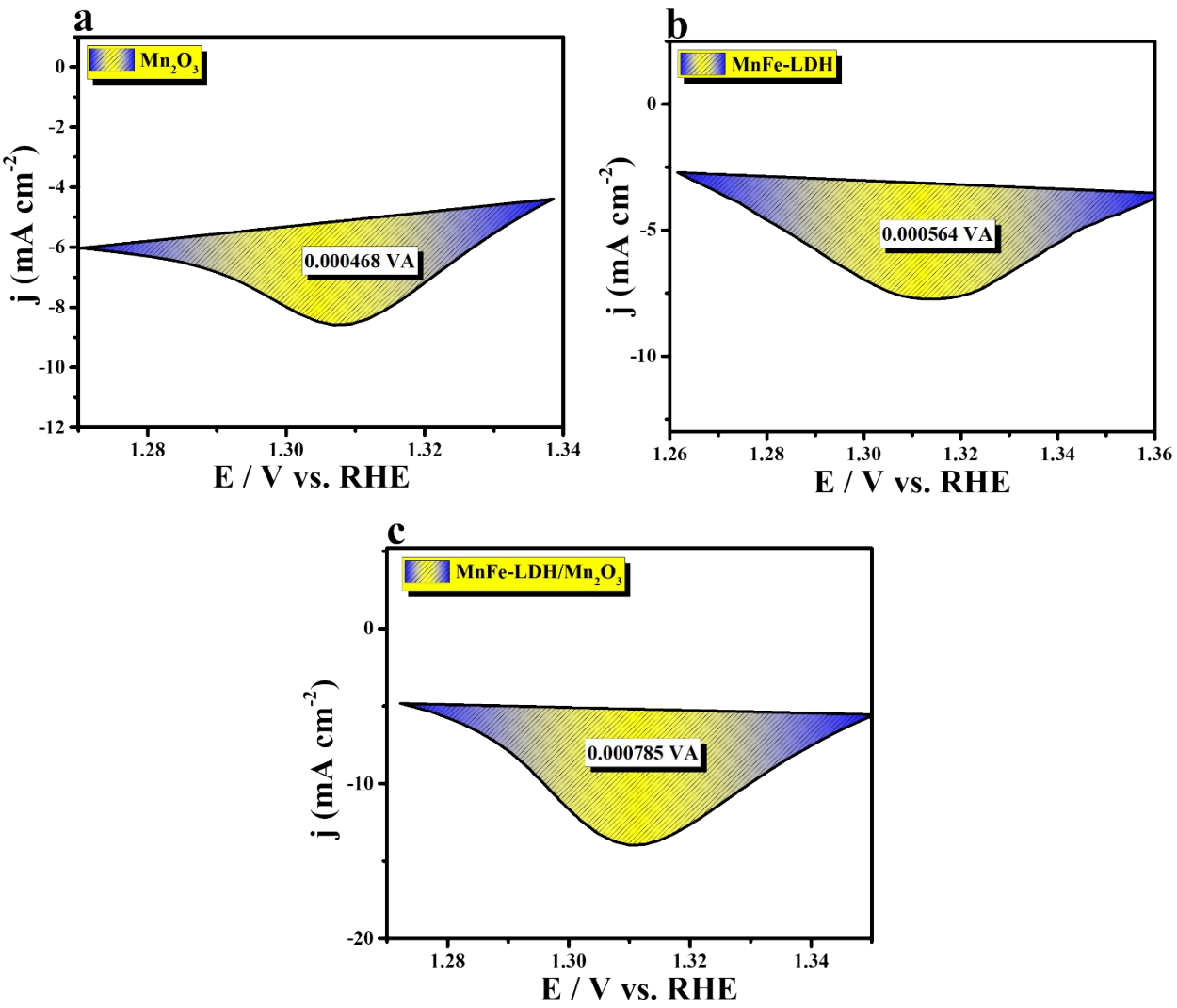

Figure S6: **(a-c)** The area of reduction peak for Mn_2O_3/NF, MnFe-LDH and MnFe-LDH/Mn_2O_3/NF respectively.

Determination of various Surface concentration in Mn_2O_3 from the redox features of CV:

Calculated area associated with the reduction of Mn^{3+} to Mn^{2+} of Mn_2O_3

$$= 0.000468 \text{ VA}$$

Hence, the associated charge is = 0.468 VA / 0.005 Vs^{-1} ⟶ **(Equation 6)**

$$= 0.0936 \text{ As}$$

$$= \mathbf{93.6\ C}$$

Now, the number of electrons transferred is

$$= 0.0936 \text{ C} / 1.602 \times 10^{-19} \text{ C} \longrightarrow \textbf{(Equation 7)}$$

$$= \mathbf{5.840 \times 10^{17}}$$

Since, the reduction of Mn^{3+} to Mn^{2+} is a single electron transfer reaction, the number electron calculated above is exactly the same as the number of surface-active sites.

Hence, the number of Mn participate in OER is = $\mathbf{5.840 \times 10^{17}}$

Hence, Determination of Turnover Frequency (TOF) from OER Current Density TOF in our study was calculated assuming that the surface-active Mn atoms that had undergone the redox reaction just before onset of OER only participated in OER electrocatalysis. The corresponding expression is,

$$TOF = j \times N_A / F \times n \times \Gamma \longrightarrow \textbf{(Equation 8)}$$

Where, j = current density N_A= Avogadro number F = Faraday constant n = Number of electrons Γ = Surface concentration.

$$TOF = [(4.4 \times 10^{-3}) (6.023 \times 10^{23})] / [(96485) (4) (5.840 \times 10^{17})$$

$$= \mathbf{0.11\ s^{-1}}$$

Calculated area associated with the reduction of Mn^{3+} to Mn^{2+} of **MnFe-LDH**

$$= 0.000564 \text{ VA}$$

Hence, the associated charge is $= 0.000564 \text{ VA} / 0.005 \text{ Vs}^{-1}$ ⟶ **(Equation 9)**

$$= 0.1128 \text{ As}$$

$$= 0.\mathbf{1128\ C}$$

Now, the number of electrons transferred is

$$= 0.1128 \text{ C} / 1.602 \times 10^{-19} \text{ C} \longrightarrow \textbf{(Equation 10)}$$

$$= \mathbf{7.0412 \times 10^{17}}$$

Since, the reduction of Mn^{3+} to Mn^{2+} is a single electron transfer reaction, the number electron calculated above is exactly the same as the number of surface-active sites.

Hence, the number of Mn participating in OER is = $\mathbf{7.0412 \times 10^{17}}$

Hence, the Determination of Turnover Frequency (TOF) from OER Current Density TOF in our study was calculated assuming that the surface-active Mn atoms that had undergone the redox reaction just before onset of OER only participated in OER electrocatalysis. The corresponding expression is,

$$TOF = j \times N_A / F \times n \times \Gamma \longrightarrow \textbf{(Equation 11)}$$

Where, j = current density N_A= Avogadro number F = Faraday constant n = Number of electrons Γ = Surface concentration.

$$TOF = [(7.4 \times 10^{-3}) (6.023 \times 10^{23})] / [(96485) (4) (7.0412 \times 10^{17})$$

$$= \mathbf{0.16\ s^{-1}}$$

Calculated area associated with the reduction of Mn^{3+} to Mn^{2+} of MnFe-LDH/Mn_2O_3

$$= 0.000785\ VA$$

Hence, the associated charge is = 0.000785 VA / 0.005 Vs^{-1} ⟶ **(Equation 12)**

$$= 0.157\ As$$

$$= 0.\mathbf{157\ C}$$

Now, the number of electrons transferred is

$$= 0.157\ C / 1.602 \times 10^{-19}\ C \longrightarrow \textbf{(Equation 13)}$$

$$= \mathbf{9.8\times 10^{17}}$$

Since, the reduction of Mn^{3+} to Mn^{2+} is a single electron transfer reaction, the number electron calculated above is exactly the same as the number of surface-active sites.

Hence, the number of Mn participating in OER is = $\mathbf{9.821\times 10^{17}}$

Hence, the Determination of Turnover Frequency (TOF) from OER Current Density TOF in our study was calculated assuming that the surface-active Mn atoms that had undergone the redox reaction just before onset of OER only participated in OER electrocatalysis. The corresponding expression is,

$$TOF = j \times N_A / F \times n \times \Gamma \longrightarrow \textbf{(Equation 14)}$$

Where, j = current density N_A= Avogadro number F = Faraday constant n = Number of electrons Γ = Surface concentration.

$$TOF = [(294 \times 10^{-3})\ (6.023\times 10^{23})] / [(96485)\ (4)\ (9.824\times 10^{17})$$

$$= \mathbf{0.47\ s^{-1}}$$

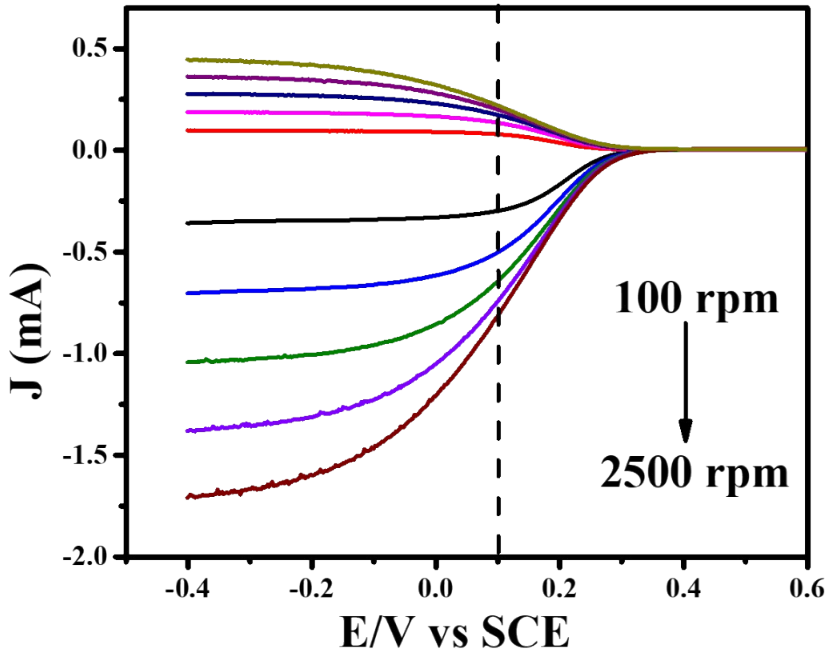

Figure S7: LSV responses of the taken RRD electrode for the redox reaction of ferro-ferri in 0.1 M KNO_3 with 10 mM of $K_3[Fe(CN)_6]$ at various rotation speed by using RRD electrode.

Table S2: Collection Efficiency (N) value for the redox reaction of ferro-ferri in 0.1 M KNO_3 with 10 mM of $K_3[Fe(CN)_6]$ at various rotation speed by RRD electrode.

S.No	Rotation speed (RPM)	Disc current (mA)	Ring current (mA)	Collection Efficiency (N)
1	100	0.297	0.074	0.249158249
2	400	0.505	0.125	0.247524752
3	900	0.637	0.157	0.246467818
4	1600	0.747	0.184	0.246318608
5	2500	0.857	0.212	0.247374562
			Average	0.247368

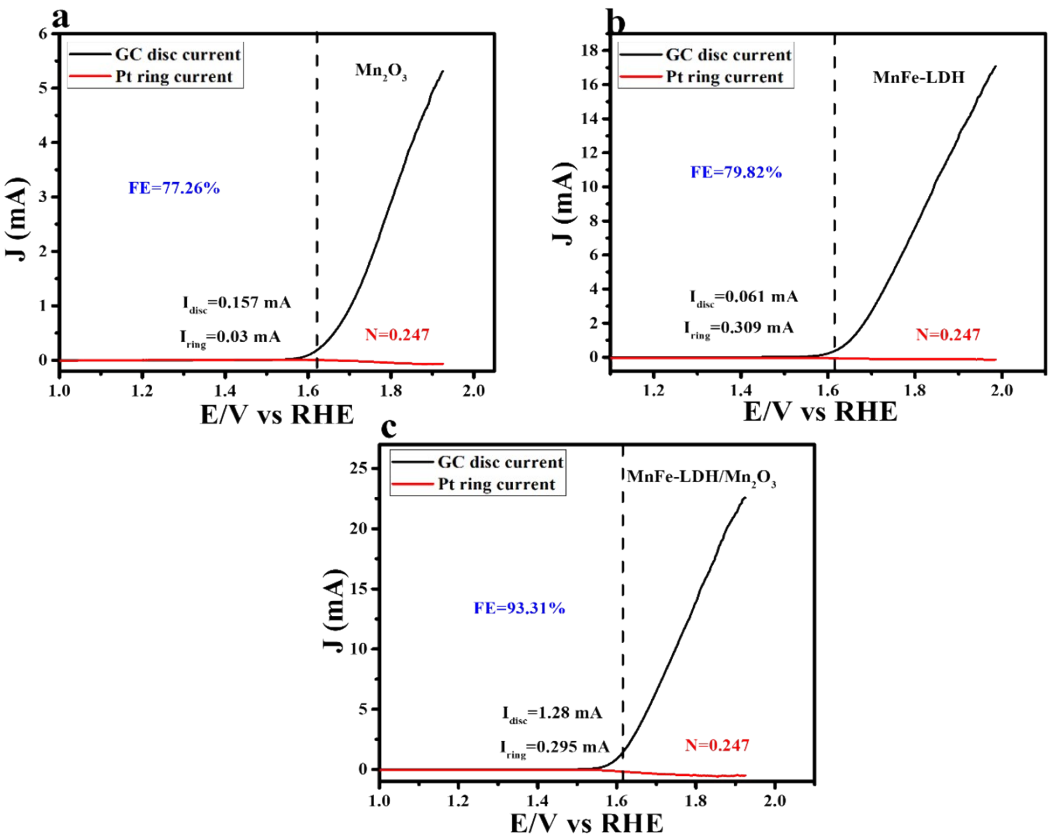

Figure S8: Linear sweep voltammetric response of (a) Mn_2O_3, (b) MnFe-LDH and (c) MnFe-LDH/Mn_2O_3 in disk electrode for OER, and corresponding ring current information for ORR. Collection efficiency (N) is equal to 0.247.

Calculation of Faradaic Efficiency (FE):

The Faradaic Efficiency for Mn_2O_3 in OER process was calculated by using Rotating Ring-Disk (RRD) technique as follows:

Ring current for complex 1 (I_{ring}) = 0.03 mA

Disc current for complex 1 (I_{disc}) = 0.157 mA

Collection Efficiency (N) = 0.247 (The Collection Efficiency (N) value calculated experimentally by using ferri/ferrocyanide system in 0.1 M KNO_3 with 10 mM $K_3[Fe(CN)_6]$, the data are given in **Figure S7** and **Table S2**)

Faradaic Efficiency in Mn_2O_3 in OER process

$$= \frac{I_{ring}}{N * I_{disc}} = \frac{0.03\ mA}{0.247 *\ 0.157\ mA} = 0.7726 *100 =$$

77.26%

The Faradaic Efficiency for MnFe-LDH in OER process was calculated by using the Rotating Ring-Disk (RRD) technique as follows:

Ring current for complex 1 (I_{ring}) = 0.061 mA

Disc current for complex 1 (I_{disc}) = 0.309 mA

Collection Efficiency (N) = 0.247

Faradaic Efficiency in MnFe-LDH in OER process

$$= \frac{I_{ring}}{N * I_{disc}} = \frac{0.061\ mA}{0.249 *\ 0.309\ mA} = 0.777 *100 = 77.7$$

The Faradaic Efficiency for MnFe-LDH/Mn_2O_3 in OER process was calculated by using the Rotating Ring-Disk (RRD) technique as follows:

Ring current for complex 1 (I_{ring}) = 0.295 mA

Disc current for complex 1 (I_{disc}) = 1.28 mA

Collection Efficiency (N) = 0.247

Faradaic Efficiency in MnFe-LDH/Mn_2O_3 in OER process

$$= \frac{I_{ring}}{N * I_{disc}} = \frac{0.295\ mA}{0.247 *\ 1.28\ mA} = 0.9331 *100 =$$

93.31%

Faradaic Efficiency of MnFe-LDH/Mn_2O_3 for other catalytic process can be calculated as follows:

Faradaic Efficiency for other catalytic process possibly catalytic activation, formation of hydrogen peroxide, and catalytic corrosion in MnFe-LDH/Mn_2O_3

=100 % - Faradaic Efficiency for other catalytic process in MnFe-LDH/Mn_2O_3
=100 % -93.31% = 7.2%

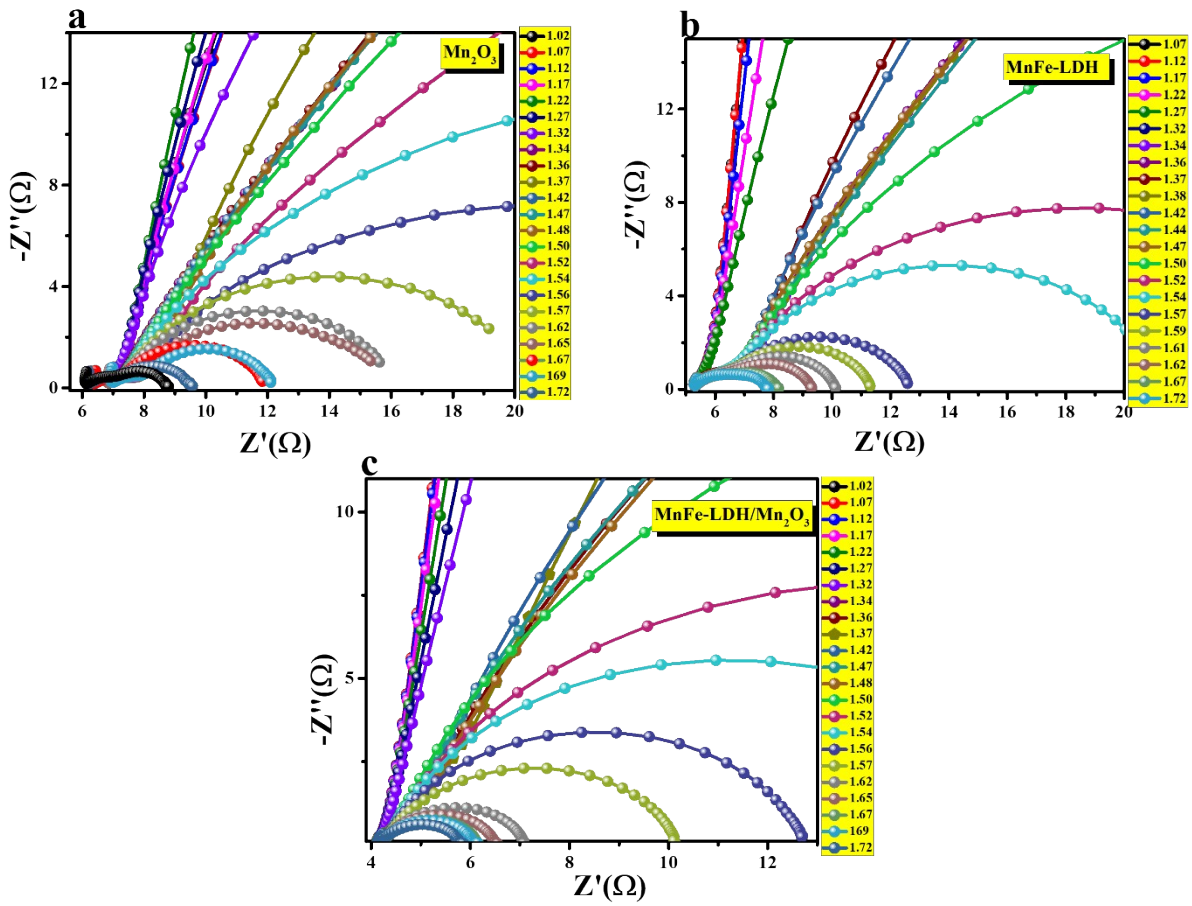

Figure S9: (a-c) Nyquist plot measured at various applied voltages of Mn_2O_3, MnFe-LDH and MnFe-LDH /Mn_2O_3 respectively.

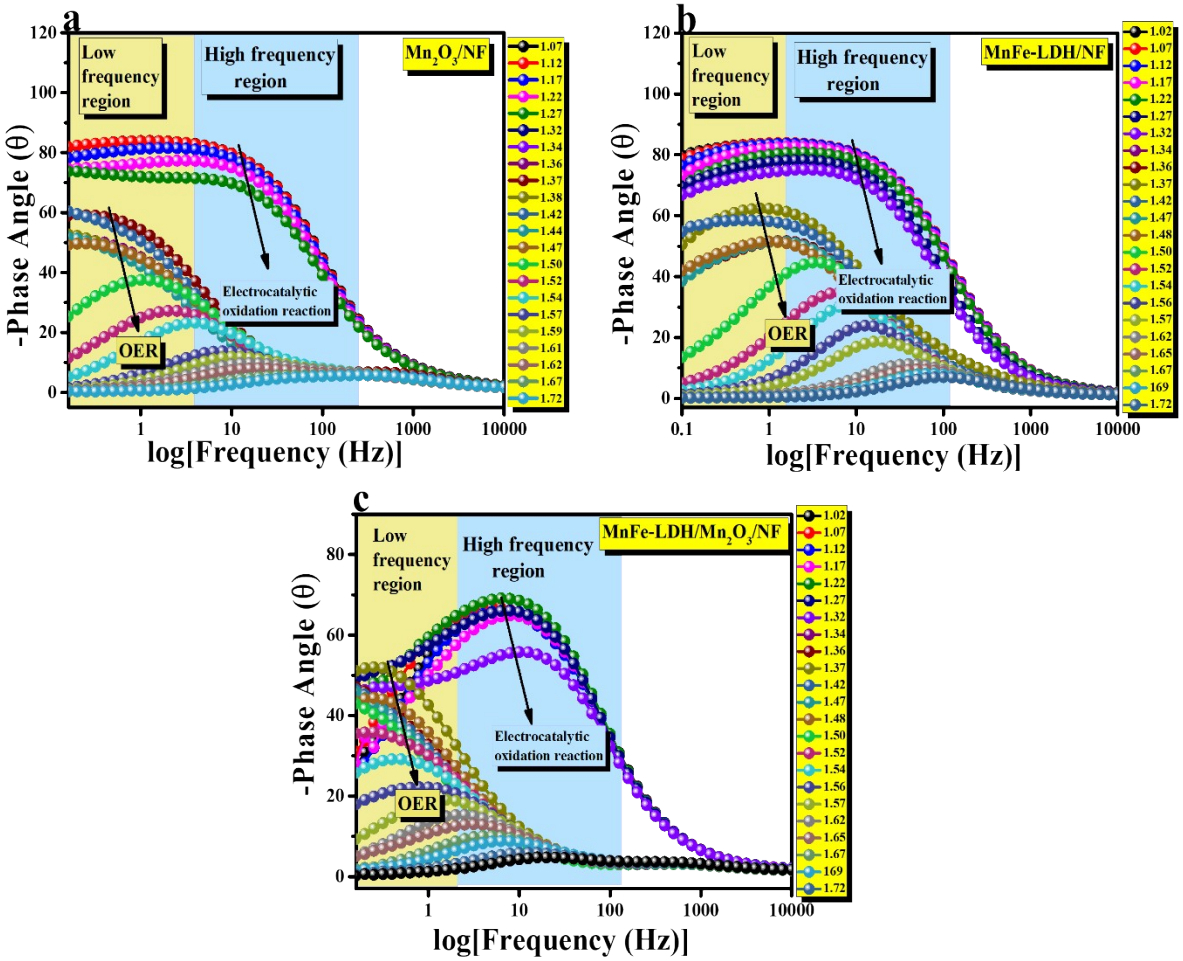

Figure S10: (a-c) Bode plot of Mn_2O_3, MnFe-LDH and MnFe-LDH/Mn_2O_3

Table S3: Comparison table for OER activity of MnFe-LDH/Mn_2O_3/NF with the similar type of catalyst.

S.No	Catalyst	Electrolyte	Overpotential (mV) @ 10 $mAcm^{-2}$	Tafel value ($mV\ dec^{-1}$)	OER Stability	Reference
1	A bio-derived carbon/MnFe-LDH (MnFe–C)	1 M KOH	280	86	25	[4]
2	B-CQDs/MnFeSe/NF	1 M KOH	197	74.61	21	[5]
3	Mo-$NiSe_2$/$CoSe_2$/NF	1 M KOH	270	49	24	[6]
4	$MnNiCoS_2$/NF	1 M KOH	310	120	42	[7]
5	FeMn-LDH/MoS_2	1 M KOH	222	33.3	25	[8]
6	D-NiMn LDH/FeS	1 M KOH	184	49	26	[9]
7	NiCoMnFe–P	1 M KOH	279	53.1	17	[10]
8	NiSe@MnFe-LDH/NF	1 M KOH	244	53.6	15	[11]
9	MnNi-LDH/Ni Foam	1 M KOH	327	61	24	[12]
10	**MnFeLDH/Mn_2O_3/NF/**	**1 M KOH**	**280**	**114**	**36**	**our work**

Table S4: Comparison table for HER activity of MnFe-LDH/Mn_2O_3/NF with the similar type of catalyst.

S.No	Catalyst	Electrolyte	Over Potential (mV)@ 10 $mAcm^{-2}$	Tafel value ($mVdec^{-1}$)	Reference
1	A bio-derived carbon/MnFe-LDH (MnFe–C)	1 M KOH	120	92	[4]
2	B-CQDs/MnFeSe/NF	1 M KOH	89	99.6	[5]
3	Mo-$NiSe_2$/$CoSe_2$/NF	1 M KOH	99	85	[6]
4	$MnNiCoS_2$/NF	1 M KOH	100	75	[7]
5	FeMn-LDH/MoS_2	1 M KOH	120	112	[8]
6	D-NiMn LDH/FeS	1 M KOH	184	49	[9]
7	NiCoMnFe–P	1 M KOH	140	116.9	[10]
8	NiSe@MnFe-LDH/NF	1 M KOH	193	74.3	[11]
9	MnNi-LDH/Ni Foam	1 M KOH	327	110	[12]
10	**MnFeLDH/Mn_2O_3/NF**	**1 M KOH**	**66**	**86**	**our work**

Table S5: Comparison table for Total water splitting of MnFe-LDH/Mn_2O_3/NF with the similar type of catalyst.

S.No	Catalyst	Electrolyte	Water splitting Voltage(V)	Current Density ($mAcm^{-2}$)	Reference
1	A bio-derived carbon/MnFe-LDH (MnFe–C)	1 M KOH	1.60	10	[4]
2	B-CQDs/MnFeSe/NF	1 M KOH	1.52	10	[5]
3	Mo-$NiSe_2$/$CoSe_2$/NF	1 M KOH	1.51	10	[6]
4	$MnNiCoS_2$/NF	1 M KOH	1.49	10	[7]
5	FeMn-LDH/MoS_2	1 M KOH	1.64	10	[8]
6	D-NiMn LDH/FeS	1 M KOH	1.50	10	[9]
7	NiCoMnFe–P	1 M KOH	1.7	10	[10]
8	NiSe@MnFe-LDH/NF	1 M KOH	1.51	10	[11]
9	MnNi LDH/Ni Foam	1 M KOH	1.85	10	[12]
10	**MnFe-LDH/Mn_2O_3/NF/**	**1 M KOH**	**1.56**	**10**	**our work**

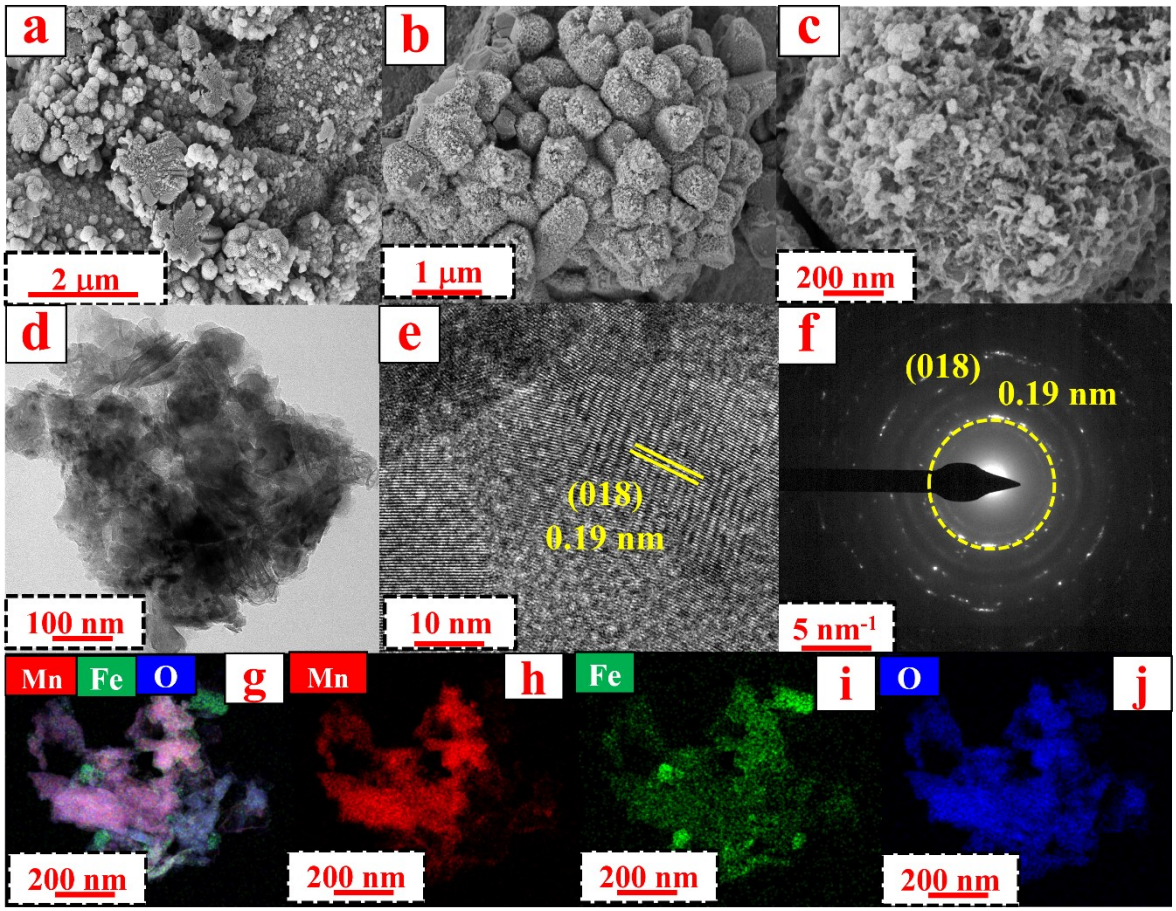

Figure S11: (a-c) Low and high magnification FE-SEM images post-OER MnFe-LDH/Mn_2O_3 respectively.: (d) HRTEM images (e) Lattice fringes (f) SAED pattern (g) HAADF color mapping (h-j) Uniform distribution Mn, Fe, and O respectively of Post-OER MnFe-LDH/Mn_2O.

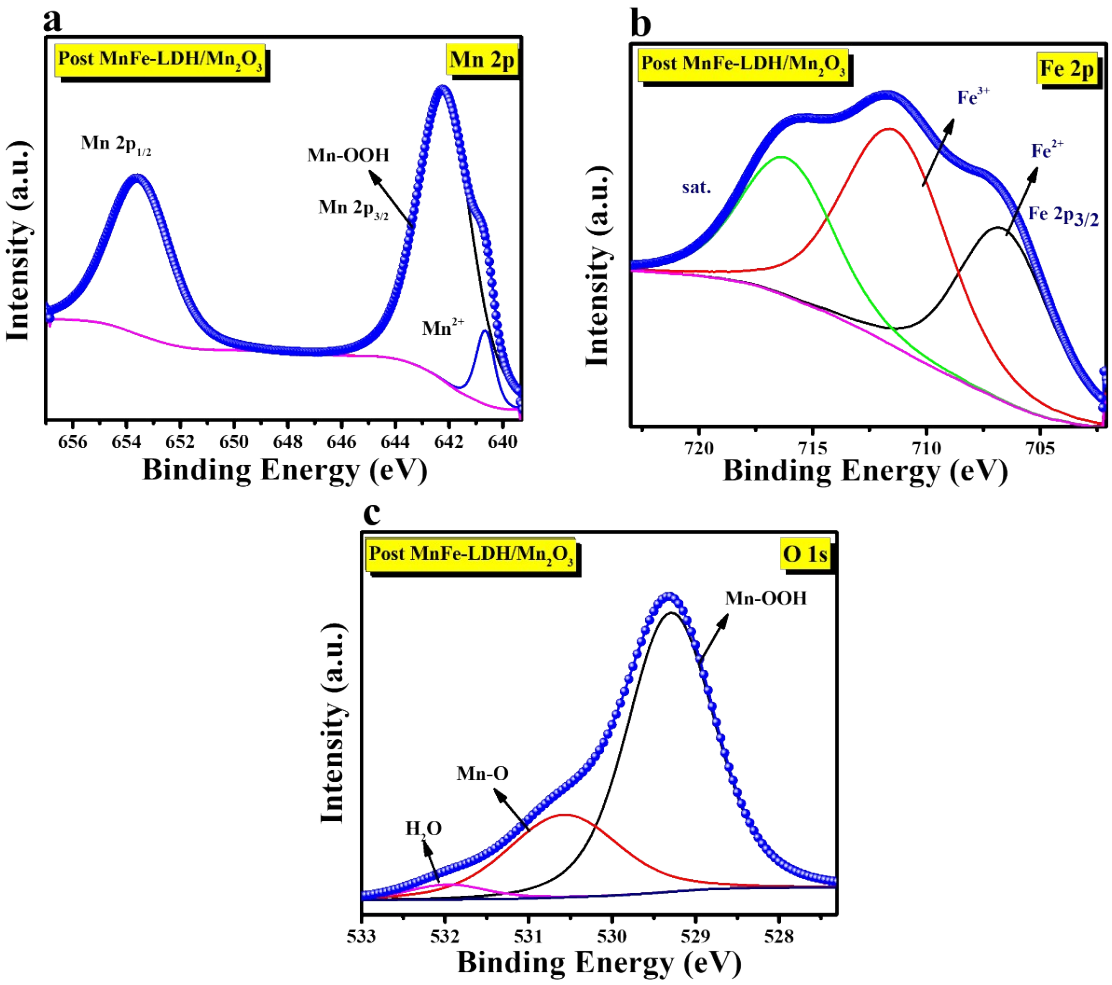

Figure S12: (a-c) The Deconvoluted XPS spectra for Mn 2p, Fe 2p and O 1s orbitals respectively for post-OER study of MnFe-LDH/Mn_2O_3.

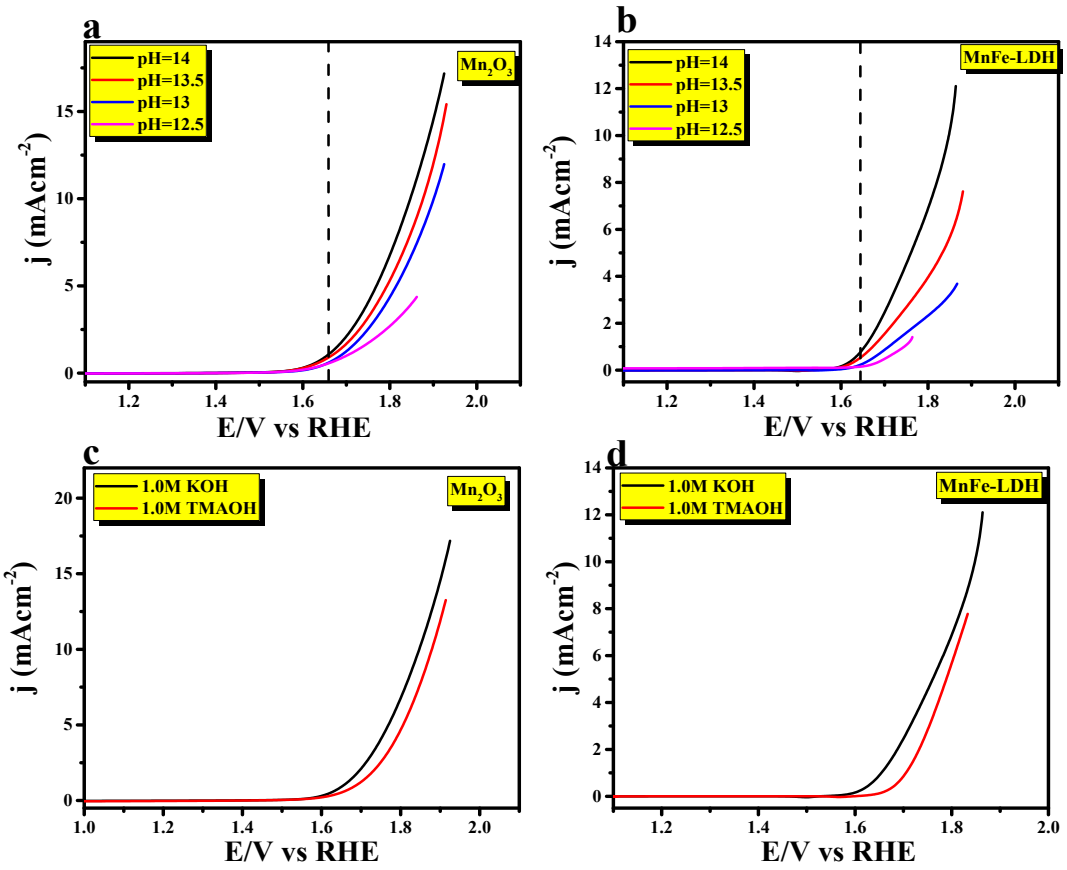

Figure S13: (a and b) LSV study of Mn_2O_3 and MnFe-LDH at various pH of KOH (c and d) LSV study of Mn_2O_3 and MnFe-LDH at 1.0 M KOH and 1.0 M TMAOH respectively.

References:

1 H. N. Dhandapani, D. Mahendiran, A. Karmakar, P. Devi, S. Nagappan, R. Madhu, K. Bera, P. Murugan, B. R. Babu and S. Kundu, *J. Mater. Chem. A Mater.*, 2022, **10**, 17488–17500.

2 E. M. Manohar, H. N. Dhandapani, S. Roy, R. Pełka, M. Rams, P. Konieczny, S. Tothadi, S. Kundu, A. Dey and S. Das, *Inorg. Chem*., 2024, **63**, 4883–4897.

3 R. Madhu, J. Muthukumar, P. Arunachalam, P. Gudlur and S. Kundu, *The Journal of Physical Chemistry C*, 2024, **128**, 12891–12902.

4 A. Mariappan, R. K. Dharman, T. H. Oh, S. Prabu and K. Y. Chiang, *Mater. Chem. Phys.*, 2023, **309**, 128321.

5 W. Zhang, M. Guo, D.-F. Chai, G. Dong, L. Bai, Z. Zhang, X. Zhang and D. Guo, *Int. J. Hydrogen Energy*, 2025, **99**, 485–493.

6 P. Aggarwal, D. Sarkar, P. K. Dwivedi, P. W. Menezes and K. Awasthi, *Int. J. Hydrogen Energy*, 2025, **171**, 151215.

7 W. Xia, X. Luan, W. Zhang and D. Wu, *Int. J. Hydrogen Energy*, 2023, **48**, 27631–27641.

8 S. Kumar, S. Raju, S. Marappa, M. S, V. D R, D. M and B. H, *ACS Appl. Energy Mater.*, 2024, **7**, 9872–9881.

9 M. Sun and J. Wang, *J. Mater. Chem. A Mater.*, 2023, **11**, 21420–21428.

10 N. K. Allam, *ECS Meeting Abstracts*, 2024, **MA2024-01**, 1857–1857.

11 Z. Pan, Z. Tang, M. Yaseen and Y. Zhan, *ACS Appl. Nano Mater.*, 2022, **5**, 16793–16803.

12 R. Srivastava, S. Bhardwaj, A. Kumar, A. N. Robinson, J. Sultana, S. R. Mishra, F. Perez and R. K. Gupta, *Int. J. Hydrogen Energy*, 2024, **49**, 971–983.